Solubility and Diffusion in Latex Films Formed from High Glass Transition Temperature Particles

Ş. UĞUR, Ö. PEKCAN

İstanbul Technical University, Department of Physics, 80626, Maslak İstanbul, Turkey

Received 25 July 1997; accepted 30 January 1998

ABSTRACT: *In situ* steady-state fluorescence measurements were used to study the dissolution of polymer films. These films were formed from pyrene labeled poly(methyl methacrylate) (PMMA) latex particles that were sterically stabilized by polyisobutylene. Annealing was performed above the glass transition temperature at 180°C at 1-h time intervals for film formation. Desorption of pyrene labeled PMMA chains was monitored in real time by the change of pyrene fluorescence intensity. Dissolution experiments were performed in various solvents with different solubility parameters, δ, at room temperature. Diffusion coefficients, D, in various solvents were measured and found to be around 10^{-10} cm^2/s. A strong relation between D and δ was observed. © 1998 John Wiley & Sons, Inc. J Appl Polym Sci 70: 1493–1502, 1998

Key words: solubility; diffusion; latex films; glass transition temperature

INTRODUCTION

Polymeric coatings are used to resist corrosion and contamination. A polymeric film can be employed for separations in a variety of membrane applications. Interest in the use of thin polymeric films in the packaging industry has grown. In controlled release applications of polymers, a solute is dispersed or molecularly dissolved in the polymer phase. In all these applications the rate of diffusion and the quality of the solvent are very important. Therefore, it is not surprising that the diffusion of solvents in solid polymers has been the subject of numerous theoretical, as well as experimental, investigations in the last 25 years.

Poly(methyl methacrylate) (PMMA) film dissolution was studied using laser interferometry by varying molecular weight and solvent quality.[1] Limm and coworkers modified the interferometric technique and studied the dissolution of fluorescence labeled PMMA films[2] by monitoring the intensity of fluorescence from the film and the interferometric signal. The solvent penetration rate into the film and the film dissolution were measured simultaneously. Fluorescence quenching and depolarization methods were used for penetration and dissolution studies in solid polymers.[3–5] The real-time, nondestructive method for monitoring small molecule diffusion in polymer films was developed.[6–9] This method is basically based on the detection of excited fluorescence dyes desorbing from a polymer film into a solution in which the film is placed. Recently, we reported a steady-state fluorescence (SSF) study on dissolution of both annealed latex film and PMMA disks using real-time monitoring of fluorescence probes.[10–12]

The mechanism of polymer film dissolution is much more complicated than small molecule dissolution. Small molecule dissolution can be explained by Fick's law of diffusion with a unique diffusion rate.[13] However, in polymeric systems many anomalies or deviations from Fick's law of diffusion are observed,[14] particularly below the glass transition

This article is dedicated to the 225th anniversary of the İstanbul Technical University.

Correspondence to: O. Pekcan.

Journal of Applied Polymer Science, Vol. 70, 1493–1502 (1998)
 CCC 0021-8995/98/081493-10

temperature (T_g) of the polymer. In general, this question of non-Fickian or anomalous diffusion can be subdivided into two subquestions. The first one concerns sorption of solvent into the glassy polymers, and the second one deals with desorption of solvents from swollen polymers. The most characteristic feature of the former is that the amount of solvent sorbed into the polymer varies with time raised to an exponent between 0.5 and 1.0; the extreme case (1.0) is called case II diffusion. The last and final step of polymer dissolution is called mutual diffusion of polymer and solvent molecules in the liquid phase.

In this work latex film samples were prepared from a dispersion of polymer colloid particles with a T_g above the drying temperature, which is called high-T latex dispersion. These particles remain essentially discrete and undeformed during the drying process. The mechanical properties of high-T powder films can be enhanced by annealing after all solvent has evaporated. The dissolution of films formed from high-T latex particles labeled with pyrene (P) dye was studied using the SSF method. These high-T particles have two components[15]: the major part, PMMA, comprises 96 mol % of the material and the minor component, polyisobutylene (PIB, 4 mol %), forms an interpenetrating network through the particle interior,[16,17] which is highly soluble in certain hydrocarbons. A thin layer of PIB covers the particle surface and provides colloidal stability by steric stabilization. Before dissolution the film samples were annealed above T_g at 180°C for 1 h. Various solvents with different solubility parameters were used as dissolution agents. *In situ* SSF experiments were performed for real-time monitoring of dissolution processes. Dissolution experiments were performed in solvents at room temperature and were designed so that P labeled PMMA chains desorbing from the swollen gel were detected by the SSF method. In order to do that direct illumination of the film sample was avoided during the *in situ* dissolution experiment. Our main goal was to create mechanically strong latex films by annealing and then study the dissolution process in various solvents to determine the relation between the diffusion (D) and solubility (δ) parameters.

EXPERIMENTAL

Latex Film Preparation

Latex particles labeled with P were prepared separately in a two-step process in which MMA in the first step was polymerized to low conversion in cyclohexane in the presence of PIB containing 2% isoprene units to promote grafting. The graft copolymer so produced served as the dispersant in the second stage of polymerization in which MMA was polymerized in a cyclohexane of the copolymer. The details were published elsewhere.[15] A stable spherical high-T dispersion of PMMA particles was produced, ranging in radius from 1 to 3 μm. A combination of ^{1}H-NMR and UV analysis indicated that these particles contained 6 mol % PIB and 0.037 mmol P groups/g polymer. (The particles were prepared in M. A. Winnik's Laboratory, University of Toronto, Toronto, Canada.)

Latex film preparation was performed by dispersing PMMA particles in heptane in a test tube where solid content was taken as 0.24%. Then films were prepared from this dispersion by placing a number of drops on 3×0.8 cm^2 glass plates and allowing the heptane to evaporate. The liquid dispersion from the droplets covered the whole surface area of the plate and remained there until the heptane evaporated. Samples were weighed before and after the film casting to determine the film thickness. The average film thicknesses were around 20 μm for all the dissolution experiments. The average size of the particles was taken as 2 μm to estimate the number of layers or the thickness of film samples. The films were annealed in an oven for 1 h above the T_g at 180°C, which was maintained within $\pm$2°C during annealing.

UV visible experiments were carried out with a Lambda 2S UV-visible spectrometer (Perkin–Elmer), and transmittance of latex films were detected between 300 and 400 nm. Scanning electron micrographs were taken at 10–15 kV in a JEOL JSM microscope. A Hummer VII sputtering system was used to gold coat the latex films.

Film Dissolution

For the dissolution experiments various solvents were chosen with different solubility parameters. Spectroscopically pure grade ethyl benzene (EB), toluene (TO), ethyl acetate (EA), benzene (BE), chloroform (CH), dichloromethane (DM), tetrahydrofuran (THF), and acetone (AC) were purchased from Merck and used as received. The characteristics of the solvents are listed in Table I.

Dissolution experiments were performed in a 1.0×1.0 cm quartz cell. This cell was placed in the spectrofluorimeter and fluorescence emission

Table I Solvent Characteristics

Solvents	Acronym	δ (cal/cm^3)$^{1/2}$	V (cm^3/mol)	D ($\times 10^{10}$ cm^2/s)	k_0 ($\times 10^2$ mg/cm^2 min)	d ($\times 10^4$ cm)
Ethyl benzene	EB	8.8	122.47	—	1.11	20.00
Toluene	TO	8.9	106.29	1.02	—	17.65
Ethyl acetate	EA	9.1	97.89	1.47	—	21.97
Benzene	BE	9.2	89.13	6.05	—	23.50
Chloroform	CH	9.3	80.17	26.40	—	21.87
Dichloromethane	DM	9.7	64.00	25.45	—	16.40
Tetrahydrofuran	THF	9.9	81.12	1.88	—	22.27
Acetone	AC	10.0	73.53	4.70	—	18.48
Polymer	PMMA	9.3	—	—	—	—

was monitored at a 90° angle so the film samples were not illuminated by the excitation light. Film samples were attached at one side of a quartz cell filled with solvent. The cell was then illuminated with 345-nm excitation light. Pyrene fluorescence intensity, I_p, was monitored during the dissolution process at 375 nm using the time drive mode of the spectrofluorimeter. Emission of P labeled polymer chains was recorded continuously at 375 nm as a function of time until there was no observable change in intensity. The dissolution cell and the film position is presented in Figure 1. Eight different dissolution experiments were run for the given solvents.

RESULTS AND DISCUSSION

It has been well established that mechanically rigid and transparent film can be formed by annealing high-T latex particles at 180°C for 1 h.[18–23] These observations are made by using the direct energy transfer method in conjunction with the SSF technique[20] and/or the direct fluorescence method.[21–23] Annealing the latex film at 130°C for 1 h causes void closure due to the viscous flow between particles.[21] Annealing the film above 130°C starts interdiffusion at the particle–particle junction where polymer chains relax across the junction surface. This process is also called equilibration in which particle boundaries start to disappear and consequently the latex film becomes mechanically strong and transparent as a result of annealing.[22,23] To illustrate these findings, scanning electron micrographs of the latex film before and after annealing at 180°C for 1 h are presented in Figure 2. Figure 2(a) shows high-T latex particles in a powder form. By annealing the latex film at 180°C, one can obtain an almost transparent film [Fig. 2(b)]. Figure 3 presents the plot of the transmitted light intensity, I_{tr}, from the latex film versus annealing temperature where 80% transparency was reached by annealing the film at 180°C for 1 h.

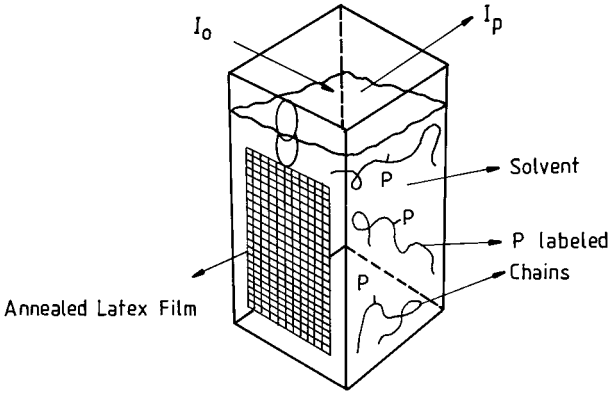

Figure 1 Dissolution cell for LS-50 Perkin–Elmer spectrofluorimeter. I_0 and I_p are the excitation and emission intensities at 345 and 375 nm, respectively.

During *in situ* dissolution experiments P labeled polymer chains were excited at 345 nm and the variation in fluorescence emission intensity was monitored with the time drive mode of the spectrofluorimeter. Figure 4 presents the P intensities, I_p, as a function of dissolution time for film samples dissolved in various solvents listed in Table I. These curves reach a plateau almost in the same fashion at long periods of time except for EB. Curves for CH and DM reached the plateau very fast, indicating quick dissolution of films. Dissolution curves for TO, EA, BE, THF, and AC are much slower than CH and DM curves. The EB curve seems to reach the plateau at very long

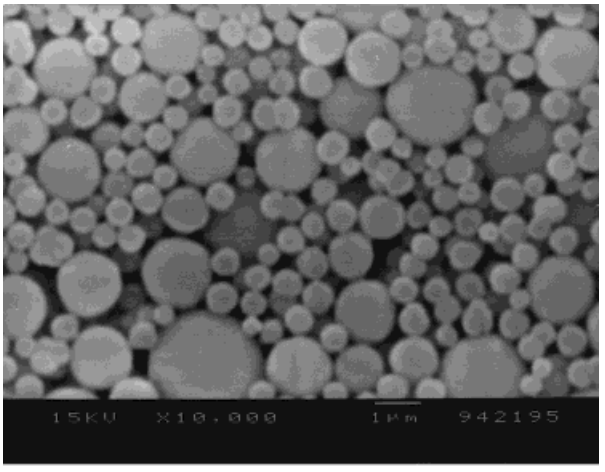

(a)

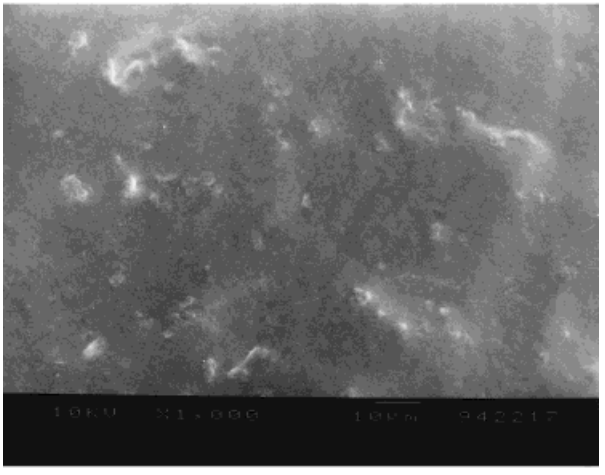

(b)

Figure 2 Scanning electron micrographs of latex film: (a) before and (b) after annealing at 180°C for 1 h.

periods of time (i.e., dissolution obeys a different diffusion model).

Phenomenon Modeling

Polymeric films dissolve mainly in three different stages: solvent diffusion, polymer relaxation, and desorption of polymer chains into the solvent reservoir. A schematic representation of these three sequential steps for the dissolution of a polymer film is presented in Figure 5. In the first stage, the penetration distance of solvent molecules mainly depends on free volume, which in turn depends on the flexibility of the chains, backbone, and side groups, as well as the thermal history of the polymer. These first solvent molecules act as a

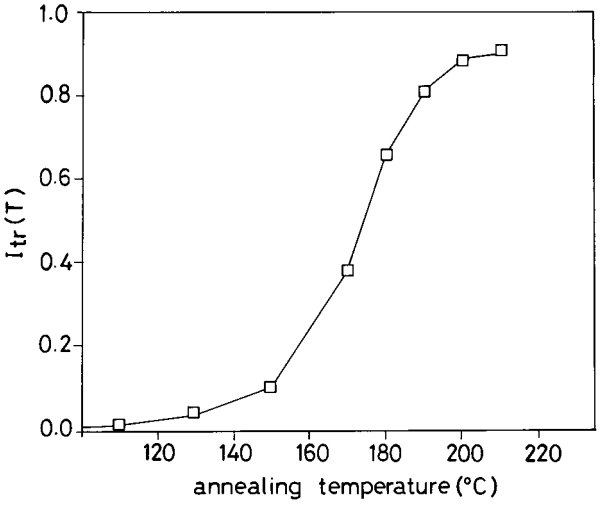

Figure 3 Plot of the transmitted light intensity, I_{tr}, from the latex film versus annealing temperature for 1-h annealing time.

plasticizer; as a result, these regions of the film start to swell. In the second stage, a gel layer is created by the relaxing polymer chains. This transition layer is composed of both polymer chains and solvent molecules. If the solvent–polymer in-

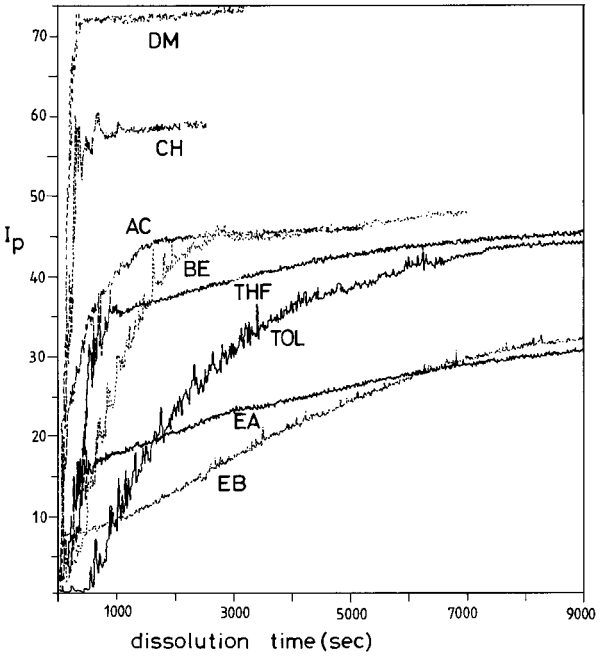

Figure 4 Pyrene intensity, I_p, versus dissolution time for the film samples dissolved in various solvents. The cell was illuminated at 345 nm during fluorescence measurements. Data for the plot were obtained using the time drive mode of the spectrofluorimeter.

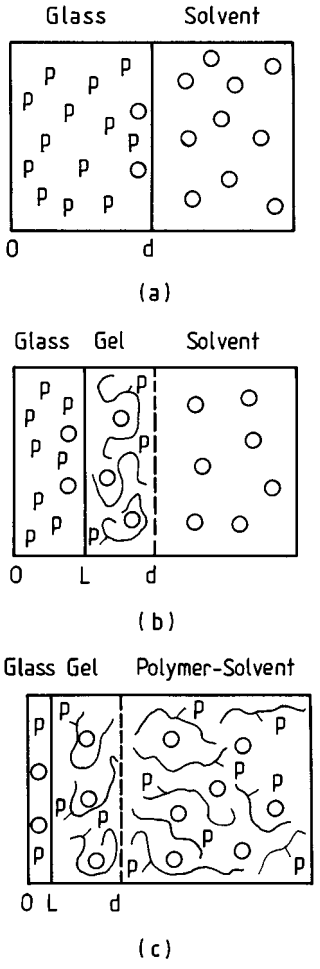

Figure 5 Stages of P labeled latex film dissolution: (a) solvent diffusion into glass, (b) formation of swollen gel, and (c) polymer desorption into solvent. Here d is the film thickness and L is the position of the advancing gel front.

teractions (solubility) are more dominant than polymer–polymer interaction, maximum swelling is obtained. This was the case when the good solvent was used during dissolution of a polymer film. In the last stage chain disentanglement takes place and chains separate from the bulk and desorb into the solvent.

Tu and Quano[24] proposed a model that includes polymer diffusion in a liquid layer adjacent to the polymer and moving of the liquid–polymer boundary. The key parameter for this model was the polymer disassociation rate, defined as the rate at which polymer chains desorb from the gel interface. Later Astaria and Sarti[25] proposed a model that explicitly considers glassy to swollen transition kinetics. Lee and Peppas[26] extended Tu and Quano's model for films to the polymer dissolution rate where gel thickness was found to be proportional to $(\text{time})^{1/2}$. A relaxation controlled model was proposed by Brochard and de Gennes[27]; after a swelling gel layer was formed, desorption of polymer from the swollen bulk was governed by the relaxation rate of the polymer stress. This rate was found to be of the same order of magnitude as the reptation time. The dependencies of the radius of gyration and the reptation time on polymer molecular weight and concentration were studied using a scaling law[28] based on the reptation model.

In this work we found it appropriate to use the model developed by Enscore et al.[29] to interpret the results of film dissolution experiments. This model includes case I and case II diffusion kinetics that are described below.

When the diffusion equation is solved in one dimension for a constant diffusion coefficient, D, and fixed boundary conditions, the sorption and desorption transport in and out of a thin slab is obtained and given by the following relation[13]:

$$\frac{M_t}{M_\infty} = 1 - \frac{8}{\pi^2} \sum_{n=0}^{\infty} \frac{1}{(2n+1)^2} \times \exp\left(\frac{-(2n+1)^2 D\pi^2 t}{d^2}\right) \quad (1)$$

Here M_t represents the amount of materials absorbed or desorbed at time t, M_∞ is the equilibrium amount of material, and d is the thickness of the slab. Equation (1) presents the model for case I diffusion, which is generally known as the Fickian diffusion.

The mechanism of case II diffusion is characterized by the following steps. As the solvent molecules enter into the polymer film, a sharp advancing boundary forms and separates the glassy part of the film from the swollen gel [see Fig. 5(b)]. This boundary moves into the film at a constant velocity. The swollen gel behind the advancing front is always at a uniform state of swelling. Now consider a cross section of a film with thickness d that is undergoing case II diffusion as in Figure 5, where L is the position of the advancing sorption front, C_0 is the equilibrium penetrant concentration and k_0 (mg/cm^2 min) is defined as the case II relaxation constant. The kinetic expression for the sorption in the film slab of an area A is given by

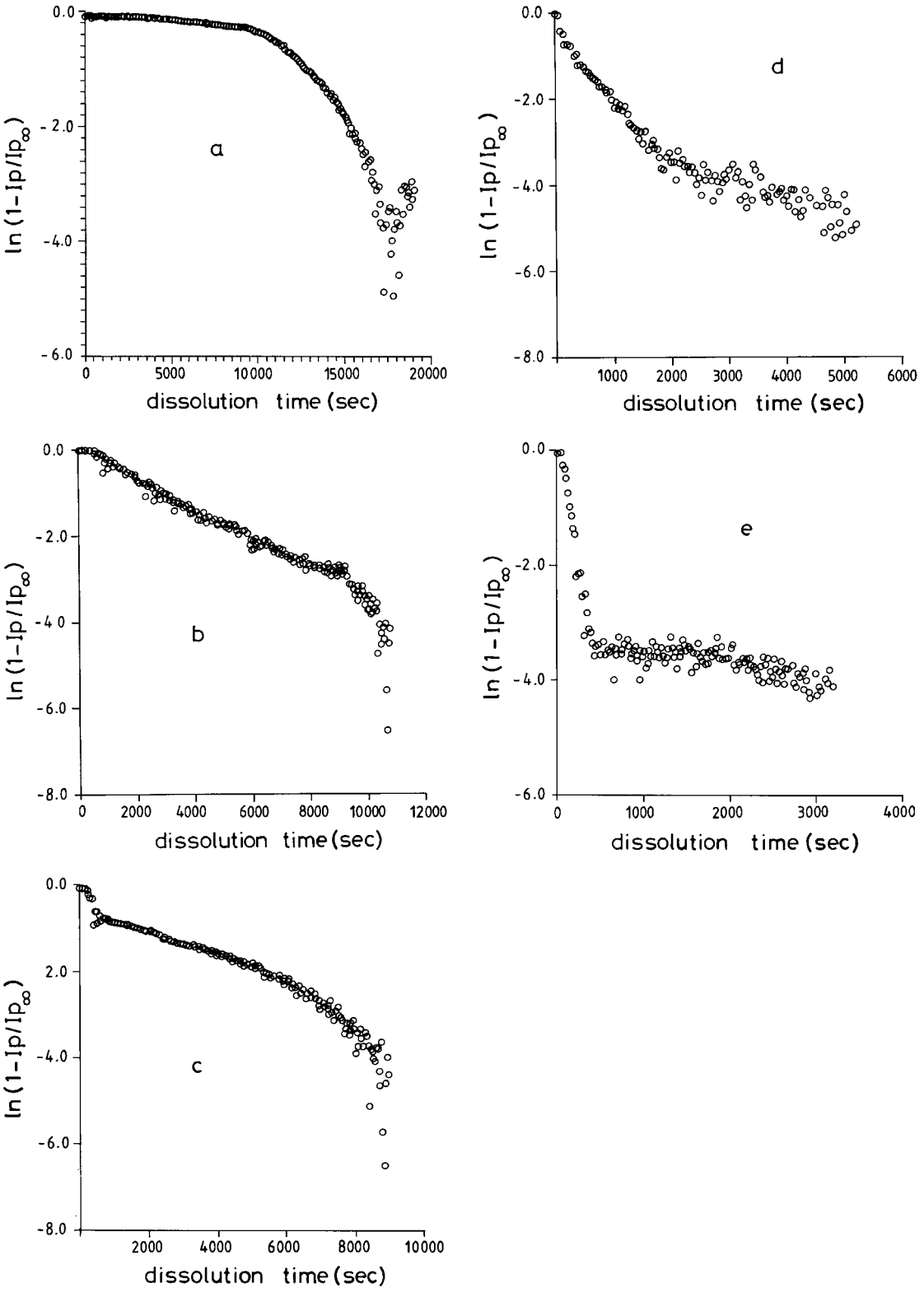

Figure 6 Plot of the digitized data in Figure 4, which obey the relation $\ln(1 - I_p/I_{p\infty}) = B - At$, where t is the dissolution time. The data are presented for samples dissolved in (a) EB, (b) TO, (c) EA, (d) AC, and (e) DM.

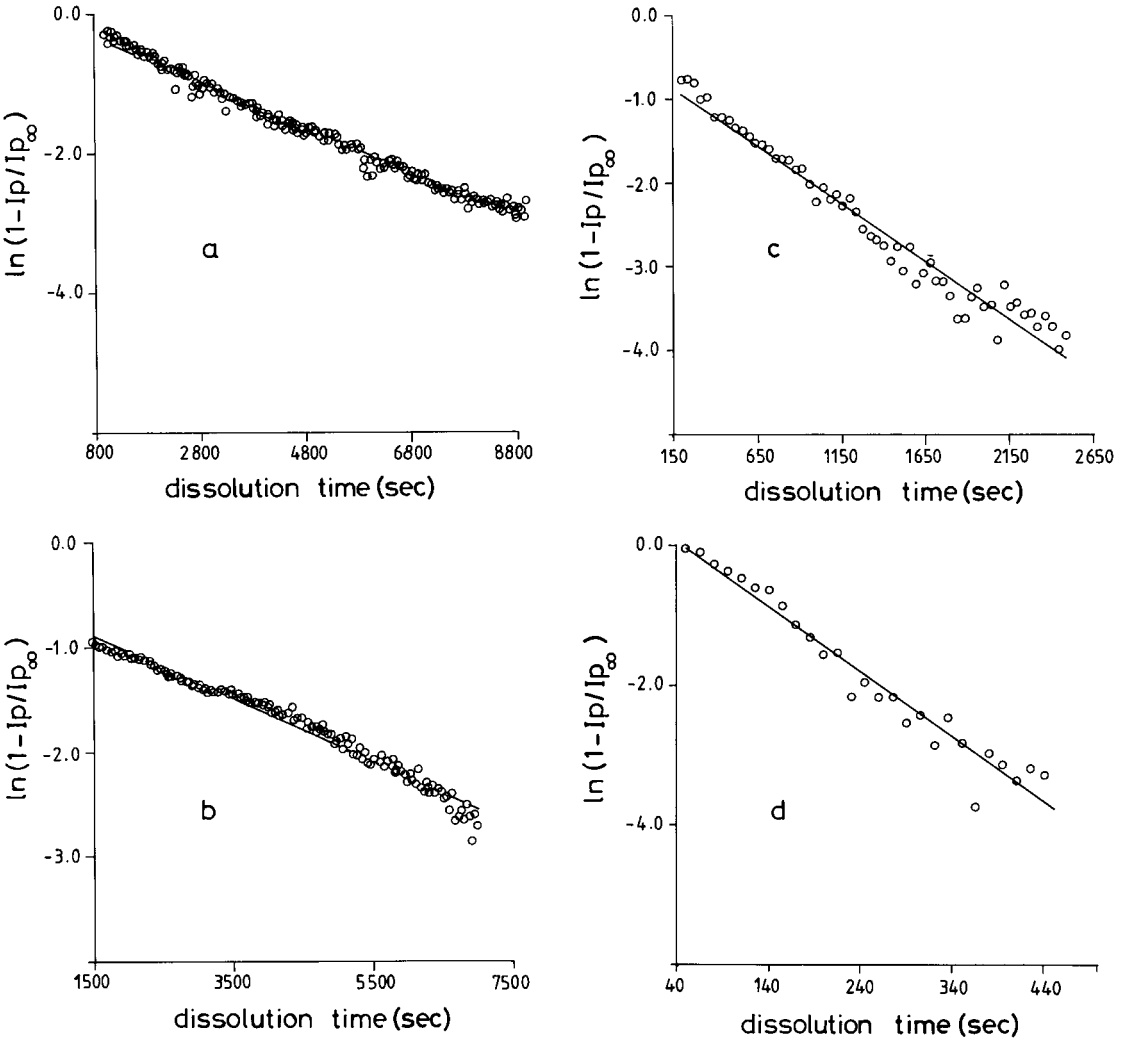

Figure 7 Comparison of the data at the linear time region presented in Figure 6(b–e) with the computations using eq. (7). Desorption coefficients, D, are obtained from the slopes of the plots for the films dissolved in (a) TO, (b) EA, (c) AC, and (d) DM.

$$\frac{dM_t}{dt} = k_0 A \tag{2}$$

The amount of penetrant, M_t, absorbed in time t will be

$$M_t = C_0 A(d - L) \tag{3}$$

After eq. (3) is substituted into eq. (2), the following relation is obtained:

$$\frac{dL}{dt} = -\frac{k_0}{C_0} \tag{4}$$

It can be seen that the relaxation front, positioned at L, moves toward the origin with a constant velocity k_0/C_0. The algebraic relation for L as a function of time t is described by eq. (5):

$$L = d - \frac{k_0}{C_0} t \tag{5}$$

Because $M_t = k_0 A t$ and $M_\infty = C_0 A d$, the following relation is obtained:

$$\frac{M_t}{M_\infty} = \frac{k_0}{C_0 d} t \tag{6}$$

The dissolution curves in Figure 4 can be quantified by fitting the data to eq. (1). Figure 6(a–e) presents the plot of the following relation for film

samples dissolved in EB, TO, EA, AC, and DM, respectively:

$$\ln\left(1 - \frac{I_p}{I_{p\infty}}\right) = B - At \tag{7}$$

This is the logarithmic form of eq. (1) for $n = 0$ with $A = D\pi^2/d^2$ and $B = \ln(8/\pi^2)$ parameters. Here, it is assumed that I_p is proportional to the number of P labeled chains desorbing from the latex film and $I_{p\infty}$ presents its value at the equilibrium condition. We must mention that the swelling process for the polymer film is too fast to be observed[10–12] for all solvents except for EB, which has a very low solubility parameter and presents the complete behavior of case II diffusion. In Figure 6 all dissolution curves are digitized for numerical treatment. Deviations from the linearity in Figure 6(b–e) at long times present equilibration of the dissolution process. The curve in Figure 6(a) for EB shows different behavior than the rest of the curves in Figure 6; this may suggest that there are at least two different mechanisms involved during dissolution of annealed high-T latex films as already discussed in the Experimental section. The linear regions of the curves at intermediate times in Figure 6(b–e) follow the Fickian diffusion model. When the linear portions of the curves in Figure 6(b–e) are compared to computations using eq. (7), chain desorption coefficients D are obtained. The linear fit of eq. (7) to the data is presented in Figure 7(a–d). The obtained D values are listed in Table I; the values for the films dissolved in CH and DM are much larger than the other solvents. When one compares the observed $D \approx 10^{-10}$ cm^2/s values with the backbone diffusion coefficient of interdiffusing polymer chains during film formation from PMMA latex particles[30,31] ($\approx 10^{-16}$–10^{-14} cm^2/s), 4–6 orders of magnitude difference can be seen. This is reasonable for the chains desorbing from swollen gel during dissolution of PMMA latex films. In fact, 10^{-10} cm^2/s is 2 orders of magnitude smaller than the D values obtained for oxygen diffusing into PMMA spheres.[32] This may suggest that penetration of solvent molecules into a latex film is almost as fast as desorption of PMMA chains from a swollen gel. Here one should realize that solvent molecules are much larger in size than oxygen molecules. Our D values (10^{-10} cm^2/s) are also similar to the D values (10^{-11} cm^2/s) obtained for n-hexane desorption from polystyrene spheres.[29]

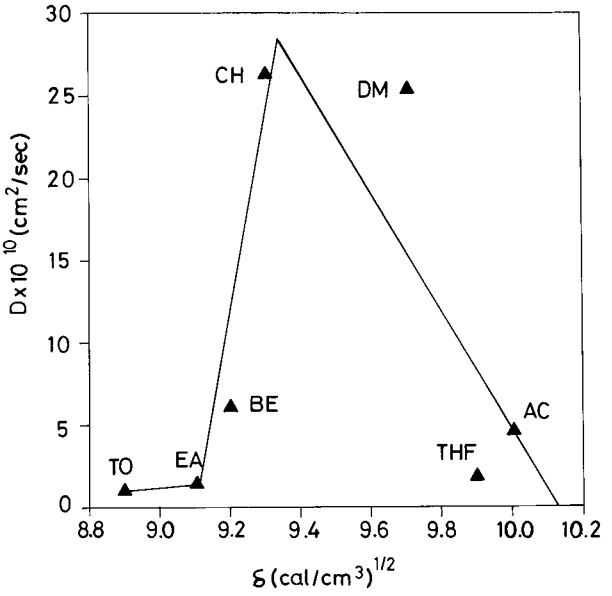

Figure 8 Plot of D versus the solubility parameter δ of solvents.

It is important to note that diffusion of solvent molecules into the latex film has a substantial dependence upon the hydrocarbon employed. The challenge is to figure out whether the kinetic effects associated with the solvent viscosity (η) or thermodynamic effect (polymer–solvent interaction) are responsible for the dissolution of the latex film. No correlation was found between η and D values. Here it is convenient to test whether the solvent quality (i.e., polymer–solvent interaction) is responsible for the dissolution processes or not. Solution theory predicts that the polymer–solvent interaction parameter is related to the solubility parameter (δ) and molar volume (V) via the following relation[33]:

$$\chi = \frac{V}{RT}(\delta - \delta_p)^2 \tag{8}$$

where R is the gas constant, T is the temperature, and δ_p is the solubility parameter of the polymer. This theory leads to the conclusion that polymers dissolve in small molecular liquids only if ($\delta - \delta_p$) is very small. A plot of D versus δ in Figure 8 shows that there is a strong correlation between χ and D values; as ($\delta - \delta_p$) approaches zero, D values present a very large number [$\delta_p = 9.3$ (cal/cm^3)$^{1/2}$ was taken for PMMA]. Here the larger D value for DM molecules most probably resulted from the smaller molar volume of this molecule.

In order to see the relation between the diffusion coefficient and molar volume, D versus V is plotted in Figure 9. From here one can conclude that the chain desorption (diffusion) coefficient is strongly correlated to the polymer–solvent interaction parameter (χ).

Non-Fickian behavior of the curve in Figure 6(a) can be interpreted by using eq. (6). When $I_p/I_{p\infty}$ is plotted as a function of dissolution time t, a reasonable linear fit was obtained for the curve in Figure 6(a). If we assume that the amount of penetrant EB molecules is proportional to the number of PMMA chains desorbing from the swollen gel, then eq. (6) can be written as

$$\frac{I_p}{I_{p\infty}} = \frac{k_0}{C_0 d}\, t \tag{9}$$

Fitting eq. (9) to the data presented in Figure 10 yielded the k_0 parameter. Using known d and C_0 (0.867 g/mL) values, the k_0 parameter was obtained and found to be 1.11×10^{-2} (mg/cm^2/min). The measured k_0 values have a 3 orders of magnitude difference from those of Enscore et al.[29] and Jacques and Hopfenberg.[34] Thus, for n-hexane sorption by polystyrene spheres and film they reported the k_0 to be around 10^{-5} mg/cm^2/min. This difference could have been caused by the stronger solvent–polymer interaction in our EB-PMMA system.

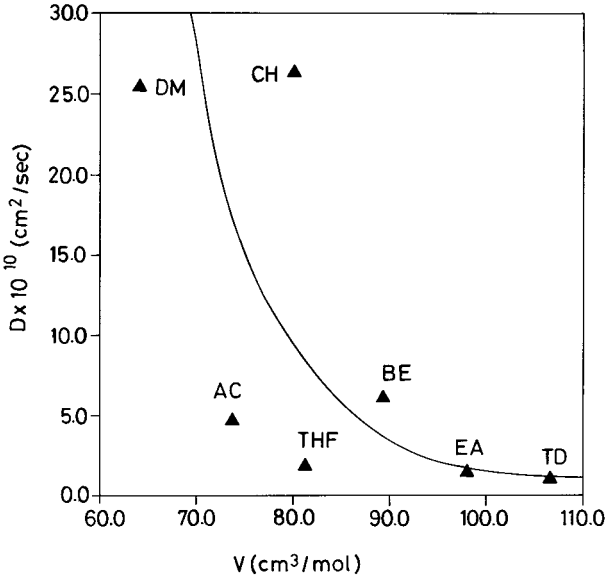

Figure 9 Plot of D versus the molar volume of solvent molecules.

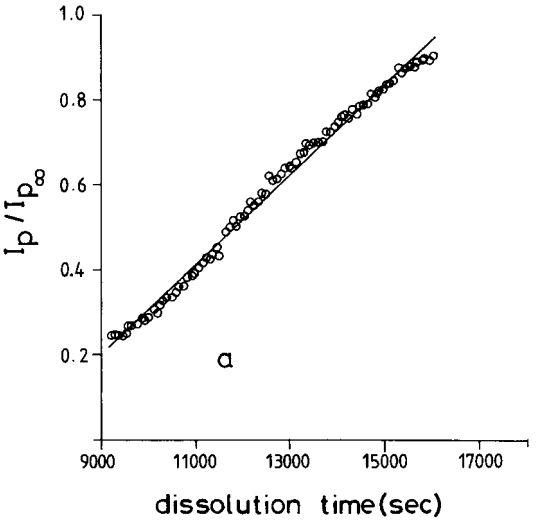

Figure 10 Comparison of the data presented in Figure 6(a) with the computation using eq. (9). The relaxation constant, k_0, is obtained from the slope.

Here the basic conclusion can be reached that the desorption (i.e., diffusion) coefficient is strictly a thermodynamic quantity that mostly associates with the solubility parameter during latex film dissolution. In other words, the rate limiting step during polymer film dissolution is the polymer–solvent interaction that may strongly affect the chain desorption from the swollen gel.

REFERENCES

1. P. D. Krasicky, R. J. Groele, and F. Rodriquez, *J. Appl. Polym. Sci.,* **35,** 641 (1988).
2. W. Limm, G. D. Dimnik, D. Stanton, M. A. Winnik, and B. Smith, *J. Appl. Polym. Sci.,* **35,** 2099 (1988).
3. J. E. Guilet, in *Photophysical and Photochemical Tools in Polymer Science,* M. A. Winnik, Ed., Reidel, Dordrecht, 1986.
4. T. Nivaggioli, F. Wank, and M. A. Winnik, *J. Phys. Chem.,* **96,** 7462 (1992).
5. D. Pascal, J. Duhamel, J. Wank, M. A. Winnik, Dh. Napper, and R. Gilbert, *Polymer,* **34,** 1134 (1993).
6. L. Lu and R. G. Weiss, *Macromolecules,* **27,** 219 (1994).
7. V. V. Krongauz, W. F. Mooney III, J. W. Palmer, and J. J. Patricia, *J. Appl. Polym. Sci.,* **56,** 1077 (1995).
8. V. V. Krongauz and R. M. Yohannan, *Polymer,* **31,** 1130 (1990).
9. Z. He, G. S. Hammond, and R. G. Weiss, *Macromolecules,* **25,** 501 (1992).
10. Ö. Pekcan, M. Canpolat, and D. Kaya, *J. Appl. Polym. Sci.,* **60,** 2105 (1996).

11. Ö. Pekcan, Ş. Uğur, and Y. Yılmaz, *Polymer,* **38,** 2183 (1997).
12. Ş. Uğur and Ö. Pekcan, *Polymer,* **38,** 5579 (1997).
13. J. Crank, *The Mathematics of Diffusion,* Clarendon Press, Oxford, U.K., 1975.
14. J. Crank and G. S. Park, *Diffusion in Polymer,* Academic, London, 1968.
15. M. A. Winnik, M. H. Hua, B. Hongham, B. Williamson, and M. D. Croucher, *Macromolecules,* **17,** 262 (1984).
16. Ö. Pekcan, M. A. Winnik, and M. D. Croucher, *Phys. Rev. Lett.,* **61,** 641 (1988).
17. (a) Ö. Pekcan, *Chem. Phys. Lett.,* **20,** 198 (1992); (b) Ö. Pekcan, *J. Appl. Polym. Sci.,* **59,** 11 (1996).
18. M. Canpolat and Ö. Pekcan, *Polymer,* **36,** 2025 (1995).
19. Ö. Pekcan, *Trends Polym. Sci.,* **2,** 236 (1994).
20. M. Canpolat and Ö. Pekcan, *J. Appl. Polym. Sci.,* **59,** 11 (1996).
21. Ö. Pekcan and M. Canpolat, *J. Appl. Polym. Sci.,* **63,** 651 (1997).
22. M. Canpolat and Ö. Pekcan, *J. Polym. Sci., Polym. Phys. Ed.,* **34,** 691 (1996).
23. M. Canpolat and Ö. Pekcan, *Polymer,* **36,** 4433 (1995).
24. Y. O. Tu and A. C. Quano, *IBM, J. Res. D,* **21,** 131 (1977).
25. G. Astaria and G. C. Sarti, *Polym. Eng. Sci.,* **18,** 388 (1978).
26. P. I. Lee and N. A. Peppas, *J. Controlled Release,* **6,** 207 (1987).
27. F. Brochard and P. G. de Gennes, *Phys. Chem. Hydrodyn.,* **4,** 313 (1983).
28. J. S. Papanu, D. S. Soane, and A. T. Bell, *J. Appl. Polym. Sci.,* **38,** 859 (1989).
29. D. J. Enscore, H. B. Hopfenberg, and V. T. Stannett, *Polymer,* **18,** 793 (1977).
30. M. A. Winnik, Ö. Pekcan, and M. D. Croucher, *Scientific Methods for the Study of Polymer Colloids and Their Applications,* F. Candau and R. H. Ottewill, Eds., Kluwer, New York, 1988.
31. Ö. Pekcan, M. A. Winnik, and M. D. Croucher, *Macromolecules,* **23,** 2673 (1990).
32. Y. Kaptan, Ö. Pekcan, and O. Güven, *J. Appl. Polym. Sci.,* **44,** 1595 (1992).
33. P. J. Flory, *Principles of Polymer Chemistry,* Cornell University Press, Ithaca, NY, 1953.
34. C. H. M. Jacques and H. B. Hopfenberg, *Polym. Eng. Sci.,* **14,** 449 (1974).